Volume 38
Number 9
September 2023
Pages 1723–1896

JAAS

Journal of Analytical Atomic Spectrometry

rsc.li/jaas

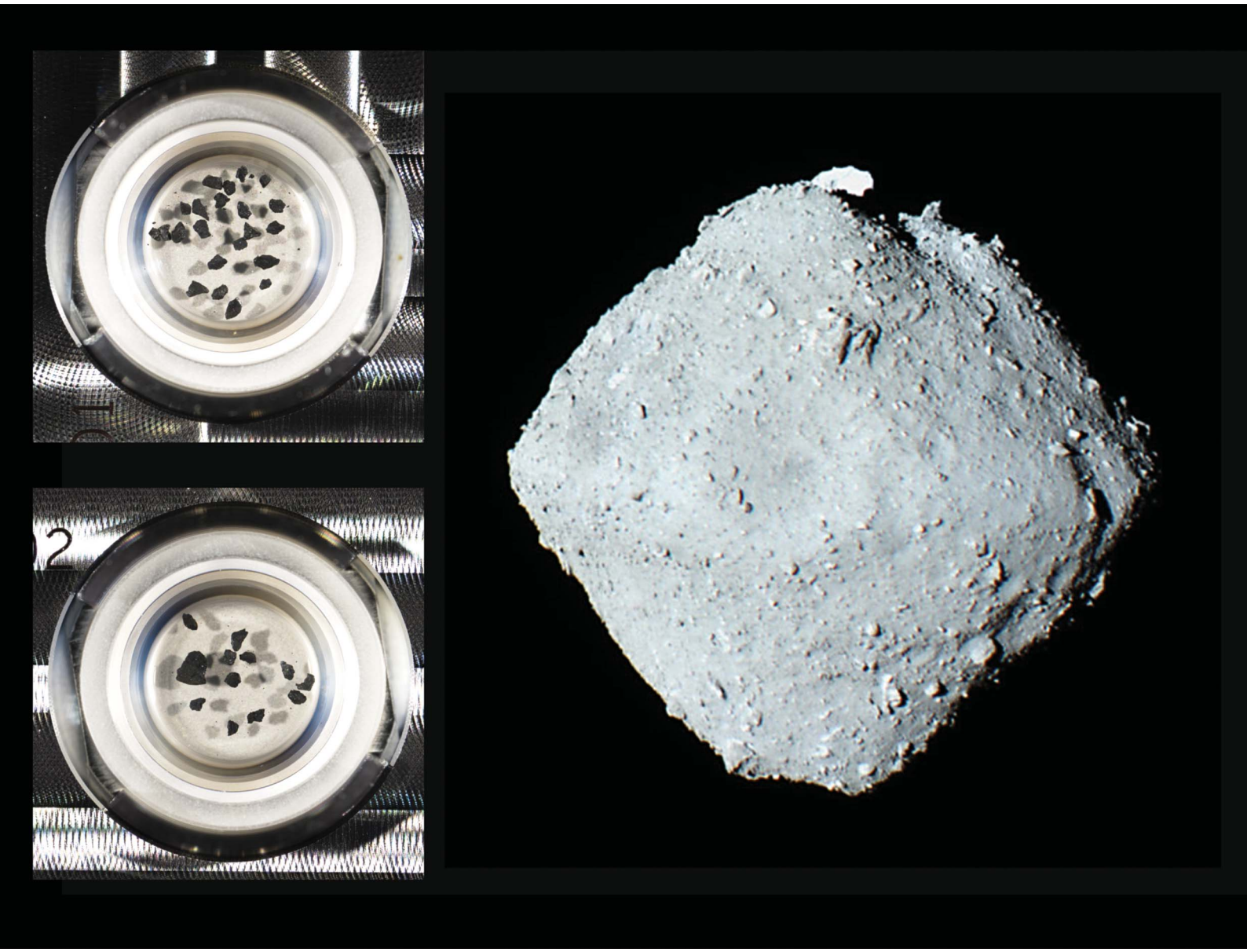

ISSN 0267-9477

ROYAL SOCIETY OF CHEMISTRY

PAPER

Alexander Meshik *et al.*
Noble gas mass-spectrometry for extraterrestrial micro-samples: analyses of asteroid matter returned by Hayabusa2 JAXA mission

JAAS

ROYAL SOCIETY OF CHEMISTRY

PAPER

View Article Online
View Journal | View Issue

Cite this: *J. Anal. At. Spectrom.*, 2023, **38**, 1785

Noble gas mass-spectrometry for extraterrestrial micro-samples: analyses of asteroid matter returned by Hayabusa2 JAXA mission†

Alexander Meshik, *[a] Olga Pravdivtseva,[a] Ryuji Okazaki,[b] Kasumi Yogata,[c] Toru Yada,[c] Fumio Kitajima,[b] Hisayoshi Yurimoto,[d] Tomoki Nakamura,[e] Takaaki Noguchi,[f] Hikaru Yabuta,[g] Hiroshi Naraoka,[b] Kanako Sakamoto,[c] Shogo Tachibana,[ch] Masahiro Nishimura,[c] Aiko Nakato,[c] Akiko Miyazaki,[c] Masanao Abe,[c] Tatsuaki Okada,[c] Tomohiro Usui,[c] Makoto Yoshikawa,[c] Takanao Sakai,[c] Satoshi Tanaka,[c] Fuyuto Terui,[i] Satoru Nakazawa,[c] Seiichiro Watanabe,[j] Yuichi Tsuda[c] and Hayabusa2 Initial Analysis Volatile Team

Mass spectrometry of noble gas isotopes extracted from limited amounts of extraterrestrial materials delivered by robotic space missions requires high sensitivity, high ion transmission, low detection limit, and several other characteristics not readily available in commercial instruments. We compared two different configurations of electron impact ionisation. We concluded that the ion source with cylindrical symmetry and without a magnetic field in the ionisation region is better for analyzing all stable noble gas isotopes extracted from sub-milligram extraterrestrial samples. Isotopic analyses of noble gases retrieved using multi-step heating of sub-mg samples delivered from near-Earth (162 173) asteroid Ryugu support this conclusion.

Received 19th April 2023
Accepted 23rd June 2023

DOI: 10.1039/d3ja00125c

rsc.li/jaas

Introduction

Noble gases and their stable isotopes are excellent geo- and cosmo-chemical tracers of geophysical processes[1] because of their very low concentrations in most natural materials. However, their chemical inertness provides a relatively easy means of separating them from major chemically active components. Noble gases can uniquely identify "presolar" (predate solar system) components that are barely resolvable by isotopes of other elements.

The Sun contains more than 99% of the total solar system mass, including the most extensive inventory of noble gases, which are omnipresent in the surface layer of all materials exposed to the Solar Wind (SW). The second most abundant noble gas component is Q (for quintessence, ref. 2), carried by the carbonaceous mineral assembly (phase-Q) in the acid-resistant residue left after HF- and HCl-dissolution of the 99.5% of the meteorite mass. The isotopic composition of heavy noble gases in phase Q resembles mass-dependently fractionated solar wind suggesting "local" (ref. 3) rather than "presolar" (ref. 4) origin. The isotopic structure of presolar noble gases differs from both solar and Q. These presolar isotopes were formed in various nucleosynthetic processes in stars and inherited by material accreted from the protoplanetary disc. Xe-HL with a U-shaped isotopic pattern due to paired excesses in both heavy and light isotopes is likely produced by the r-process (rapid neutron capture) and the p-process that generates proton-rich isotopes. Lighter noble gases (Kr, Ar, Ne, and He) co-released with Xe-HL are also labelled – HL since they seemingly have a common carbonaceous carrier in primitive meteorites – nanodiamonds. Noble gas isotopes from "presolar" silicon-carbide and graphite preserve the record of slow-neutron capture (s-process) that occurred in asymptotic giant branch (AGB) stars.[5] All above mentioned noble gases (often called "trapped") carry specific isotopic signatures

[a]*Physics Department, Washington University, Saint Louis, MO, 63130, USA. E-mail: ameshik@physics.wustl.edu*
[b]*Department of Earth and Planetary Sciences, Kyushu University, Fukuoka, 819-0395, Japan*
[c]*Institute of Space and Astronautical Science, Japan Aerospace Exploration Agency (JAXA), Sagamihara, 252-5210, Japan*
[d]*Department of Earth and Planetary Sciences, Hokkaido University, Sapporo, 060-0810, Japan*
[e]*Department of Earth Science, Tohoku University, Sendai, 980-8578, Japan*
[f]*Division of Earth and Planetary Sciences, Kyoto University, Kyoto, 606-8502, Japan*
[g]*Department of Earth and Planetary Systems Science, Hiroshima University, Higashi-Hiroshima, 739-8526, Japan*
[h]*UTokyo Organization for Planetary and Space Science, The University of Tokyo, Tokyo, 113-0033, Japan*
[i]*Kanagawa Institute of Technology, Atsugi 243-0292, Japan*
[j]*Department of Earth and Environmental Sciences, Nagoya University, Nagoya, 464-8601, Japan*

† Electronic supplementary information (ESI) available. See DOI: https://doi.org/10.1039/d3ja00125c

characteristic of their mineral hosts (reference compositions in ESI†). Other isotopes formed *in situ* have accumulated later from radioactive decay, spallation, and other nuclear reactions.[6]

Refractory minerals retain signatures of the early processes; other materials may lose nucleosynthetic noble gases to various degrees due to thermal and/or aqueous alteration. Isotopic analyses of noble gases extracted from different solar system objects reveal fingerprints of various processes that have led to their present isotopic composition and ultimately decipher the formation and evolution of the analysed materials.

Extraterrestrial materials available for (destructive) noble gas analyses are often limited or insufficient for retrieving useful information. This was the rationale for developing analytical techniques capable of reliable mass-spectrometric analyses of all noble gas isotopes from sub-mg asteroid material.

Washington University Noble Gas Laboratory (WUNGL)[7] has four operational mass spectrometers: multi-collector Noblesse (NU-Instruments), Helix-MC+ (ThermoFisher), and two nearly identical single collector instruments, one built in Zurich,[8] another cloned later in St. Louis. All instruments have magnetic sector geometry, electron impact ionization, and identical calibration systems. Three mass spectrometers can share gas extraction lines, which provides a direct comparison of their performances by analysing gas released from the same sample. This arrangement allowed us to optimize the experimental configuration for obtaining the most accurate and precise isotopic composition of all noble gases extracted from the microgram samples of the asteroid Ryugu delivered by the Hayabusa2, JAXA mission.

Methods

Sensitivity

Sensitivity is crucial for analysing small amounts of noble gases when ion counting statistics limit precision. In 1950–1960 noble gas mass-spectrometry experienced three significant advancements: (1) static vacuum mode of operation, (2) bright Nier ion source utilizing electron impact ionization, and (3) an ion-counting detection. These three innovations dramatically increased sensitivity, reducing detection limits; thus, making noble gas isotope mass spectrometry an invaluable tool for isotope geochemistry, geochronology, and nuclear physics. Since then, however, the sensitivity of noble gas mass spectrometers has remained the same. Three commercial noble gas instruments dominate the present market – Noblesse (Nu Instruments), Helix (ThermoFisher Scientific), and NGX (IsotopX). All three have the same fundamental $\sim$1 mA Torr^{-1} sensitivity as the earlier generation instruments VG-5400 and MAP-215 (when renormalized to the same electron emission current).

Since ionization cross sections and ionization potentials of the elements cannot be changed, the only way to improve the sensitivity of the ion source is to increase electron density in the ionization region by increasing the electron emission current. Increased current can be achieved by reducing work function by doping tungsten filament with some REE, or using a lanthanum hexaboride (or similar) emitter. It is feasible to further increase the path of electrons by optimizing the magnetic field configuration in the ion source, but no significant progress has been reported yet. Resonance ionization dramatically improves of sensitivity for the major Xe and Kr isotopes,[9,10] but light, low abundant isotopes are often affected by unresolvable, non-resonantly ionized hydrocarbons.[9] Hence, this elegant technique does not work for Ar, Ne, and He. Recently developed, a quadrupole ion trap mass spectrometer achieves the sensitivity of 1×10^{13} cps Torr^{-1} (ref. 11), three orders of magnitude less than the sensitivity of modern magnetic sector instruments.

Another approach is the implementation of the high-sensitivity Baur–Signer ion source with cylindrical symmetry.[12] The ring-shaped filament emits a hollow cone of electrons and does not require an electron-focusing magnet essential for operating the Nier ion source. The magnetic field in the ion-forming region bends ions of different mass/charge, introducing elemental and isotopic discrimination. The magnet-free Baur source has much smaller and more stable mass discrimination allowing to analyse all noble gases without re-tuning the ion source. It is also $\sim$4 times more sensitive than the Nier source,[12] but its sensitivity is pressure dependent. Compared to the Nier source, ions in the Baur source stay in the ionization area longer (nearly zero extraction potential), which causes undesirable space charge effects making sensitivity pressure dependent and limiting the application of the Baur source for the analyses of terrestrial samples. Later source modifications (GS 73, GS 75, and GS 98) address nonlinearity but at the expense of ion transmission and sensitivity.[12] However, for the purified gas extracted from sub-milligram natural samples, the static pressure in the mass spectrometer remains well below 10^{-9} Torr, and the ion count rate rarely exceeds 10^5 count per s (except for ^{40}Ar).

Ion transmission and consumption

Ion transmission — the fraction of ionized atoms passed through the instrument and counted by the detector — is another crucial factor in analyses of small gas amounts. High transmission is needed to minimize an instrumental bias, mass discrimination, that "must vanish as the transmission approaches 100%".[13] Nier-type ion sources typically have less than 20% ion transmission. Even in "bright" sources, only one of every five ions is detected. In contrast, the Baur ion source, especially its early version, has at least 90% transmission.[12]

Other factors to consider for micro-analyses of noble gases include gas consumption during the measurements and memory effects. In static vacuum mode, a mass-spectrometer acts like an ion pump. During the measurements, the count rates steadily decrease due to ion implantation into the detector and beam-defining electrodes. Newly ionized atoms of noble and chemically active gases can knock out previously implanted ions, increasing the count rate with time. When the contributions of these two counteracting processes are compatible, the time evolution of the count rate becomes non-monotonic. As a result, the count rate needs to be approximated by two superimposed exponents to interpolate the count rate to the beginning of the analysis (Fig. 1).

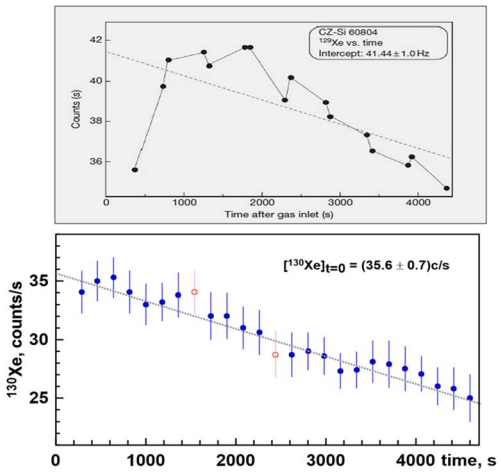

Fig. 1 Time-evolution of similar Xe signals with noticeable memory effect (top panel, copy of Fig. 3a from ref. 14). A strong memory effect causes the increase in count rate during the first three cycles. The linearly zero-extrapolated value of 41 ± 1 Hz is meaningless. The actual initial count rate is likely <36 Hz observed in the first cycle. Hence, this instrument appears have been exposed to significant quantities of Xe.[14] A Similar signal of ^{130}Xe without a noticeable memory effect is shown at the bottom panel. A linear zero-extrapolated value of 53.3 ± 0.7 Hz is most likely correct. Vertical error bars correspond to standard deviations of count rates in one measurement cycle. Total number of cycles is 25. Two data points were rejected since their corresponding ^{130}Xe/^{132}Xe ratios deviate from the fit line by more than 2.5σ.

In practice, noble gas analyses only last once all ions get counted. Although longer duration analyses would improve counting statistics, the systematic errors would increase due to the memory effects. The counting rate "half-life" determines reasonable analysis duration. In our instruments with a Baur ion source, this time is about 1 hour, while for our Helix-MC+ and Noblesse, the half-life is between 15 and 20 minutes, which significantly compromises counting statistics.

Multicollection

The early generation of noble gas mass spectrometers operated in single collection mode: only one isotope was measured at a time, while others were not counted. In this respect, the introduction of simultaneous counting of several isotopes provided a significant improvement due to better utilization of ions. There is a drawback, however. In static vacuum mode, the ion beam intensity is proportional to the partial pressure of the analysed isotope and hence inversely proportional to the internal volume of the mass-spectrometer. Therefore multi-collection comes at a price – the gain in ion collection efficiency is compromised by increased volume, making these instruments not significantly better than the traditional single-collector mass spectrometers. For example, the 5-multiplier Noblesse mass-spectrometer has about a 3 litre volume, more than three times larger than our single collector instruments.

Additionally, in multi-collector instruments, a new source of systematic error appears – variations of relative counting efficiencies of the electron multipliers. This problem is typically mitigated by shifting the magnetic field by one or two mass units; *i.e.*, the same isotope is measured by different ion detectors in the same run.[15,16] It allows directly estimating of the efficiency ratios but only between neighbouring detectors. The ratios of isotopes further apart are the product of several correction factors, which inflates analytical errors. This approach is not useful for the analyses of small ion signals.

Ion counting

Despite recent advancements in sub-femtoampere current measurement techniques,[17,18] ion counting with secondary electron multipliers remains the only practical option for small ion currents. As the count rates become lower, the pulse height distribution of the electron multiplier becomes a crucial parameter for separating a valid ion signal from the multiplier noise. The optimal pulse discrimination level depends on the mass of incoming ions[19] and should be adjusted as the multiplier ages. In an attempt to make the instrument "user-friendly", manufacturers of commercial noble gas mass-spectrometers do not necessarily provide a means to investigate pulse height distribution, *e.g.*, the ability to select and adjust the discrimination threshold depending on analysed gas. Meanwhile, for low count rate measurements, setting a correct discrimination level for analyses of different noble gases and monitoring pulse height distribution is essential to maximize counting efficiencies, reject noise, and double counting caused by pulse ringing.

In our built-in-house instruments, the operation and isotopic analyses are controlled by a flexible LabView code that allows setting an individual discrimination level for each gas and, if necessary, for each isotope. One of the routines embedded in this code is a determination of pulse height distribution (Fig. 2) that diagnoses the multiplier health and helps to determine an optimal discrimination level for each mass.

During isotopic analyses, two identical channels simultaneously count each ion beam with slightly different (by a few

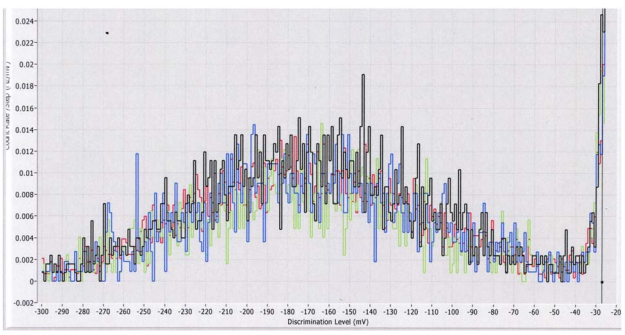

Fig. 2 Screenshot of pulse height distribution (bin size is 1 mV) for low ^{124}Xe count rate suggesting an optimal discrimination level of about −40 mV; for the most abundant ^{132}Xe it is about −60 mV. Commercial noble gas instruments cannot obtain this representation of pulse height distribution for small signals. Instead, the count rate as a function of the multiplier voltage is used. Such a plot, however, does not allow finding the optimal discrimination threshold and does not work for low count rates.

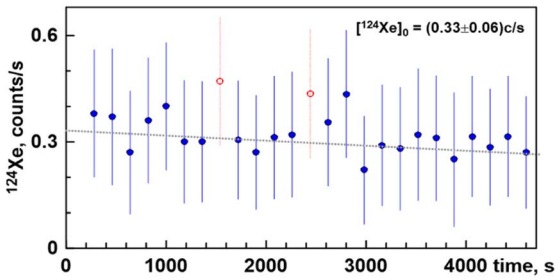

Fig. 3 Time-evolution of small signal corresponding to ~5000 atoms of ^{124}Xe. Even in this extreme case no memory ingrowth is observed. Zero-extrapolated value is 0.33 ± 0.06 counts per s. Two data points are rejected since the corresponding ^{124}Xe/^{132}Xe ratios deviate from the fit line more than 2.5σ.

mV) pulse discrimination thresholds. Although this approach does not improve the counting statistics (the same number of events), it monitors pulse height distribution change during analysis. To enhance sensitivity, we compared two discriminator settings based on the cumulative count rate of all isotopes. If these sums are within statistical errors, then the count rates for both channels are averaged. If one is significantly larger than the other, only one set of count rates is taken into account. This ion detection method makes low count rate measurements more reliable and provides early warning of possible multiplier problems – *e.g.*, degrading, aging, or dark current changes. Fig. 3 illustrates the result of our efforts to analyse minute amounts of noble gases extracted from a microgram-size sample.

Background

Minimizing experimental background is an obvious requirement for the analyses of small samples. Extraterrestrial materials from meteorites and asteroids have fresh, well degasses surfaces susceptible to the terrestrial contaminants.[20] This assertion especially applies to small particles with a high surface/volume ratio. Samples from asteroid Ryugu analysed in this work are the first extraterrestrial material that largely avoided terrestrial contamination due to careful planning and execution of the JAXA Hayabusa2 mission.[21–23] However, mass spectra always contain background signals from the intrinsic atmospheric noble gases and hydro- and fluro-carbon residual contaminants that can interfere with noble gas isotopes.

Isobaric interferences

Oils and lubricants are the primary sources of hydrocarbons in the background. Commercial mass-spectrometers typically use economical, claimed to be oil-free, turbomolecular pumps or popular tabletop pumping stations that contain an ~8 ml oil cartridge on the low vacuum side. In case of power/vacuum failure, the entire vacuum system could be easily contaminated by the oil vapours from this cartridge. We mitigate this risk using true oil-free Osaka turbopumps with magnetically levitated rotors backed by a scroll pump. The Osaka pump obtains a pressure of $<5 \times 10^{-10}$ mbar. Further pressure reduction is achieved with two 40 l s^{-1} ion pumps. All components of our vacuum systems were machined using water-soluble lubricants and acetone as cutting fluids. Whenever possible, the internal surfaces of the gas preparation line were electro-polished, and ultra-sonicated in acetone and de-ionized water. All vacuum lines are at least $\frac{3}{4}$" OD to facilitate electro-polishing and to maximize pumping speed. The entire system has been repeatedly baked to 275 °C and is constantly kept at 90 °C. Further background improvement has been achieved by utilizing a hot (>1000 °C) W-filament that cracks long hydrocarbons into smaller fragments that miniature Ti-sublimation pumps can adsorb. However, ubiquitous hydrocarbons are still present at low levels and interfere with some noble gas isotopes. Most of these interferences are only partially resolvable from Xe, with the most prominent being C_3F_5 (m/z = 131) C_9H_{20} (m/z = 128) and C_6H_6 (m/z = 78).

Other types of barely resolvable isobaric interferences are protonated peaks: HD^+ and H_3^+ from ^{3}He and $^{20}NeH^+$ from $^{21}Ne^+$; and double charged CO_2^{++} from $^{22}Ne^+$, $^{40}Ar^{++}$ from $^{20}Ne^+$. We use predetermined correction factors to account for all these interferences and measure peaks with m/z = 2, 3, 4, 18, 19, 20, 21, 22, 40, 44 in the same run. This approach is possible due to an excellent Varian Mat magnet with rapid and reproducible field stabilisation, in just a couple seconds, with little field scanning required to remove the hysteresis. Finally, there is the interference of $^{80}Kr^+$ with ^{40}Ar beam due to the so-called "change of charge" effect. Nevertheless, all Kr and Xe isotopes can be measured in the same run if Ar is not abundant or/and cryogenically separated.

The background of a clean well-baked vacuum system typically has a near atmospheric isotopic composition and usually constitutes a negligible fraction of the extracted gas. However, the background contribution (blank) can be significant and isotopically distinct when analysing a limited amount of gas. There are some peculiarities of noble gas background (blanks) that we do not entirely understand. For example, blanks made before sample fusion are sometimes larger than after the sample has been melted and presumably completely degassed. Melting a few mg of Al- or Pt-foil has the same effect on the noble gas blank. It could be that hydrogen from these foils reduces some remaining, not completely degassed surface impurities. If excessive hydrogen becomes a problem during the analysis, a Pd-filter can remove it. This approach was utilized during analyses of solar wind collectors from Genesis NASA mission.[24] Kept at ~450 °C, it effectively removed hydrogen from the vacuum system. In this work, however, we did not use this technique since it increases CO_2^{++}, which interferes with $^{22}Ne^+$ in the mass spectrum.

Noble gas extraction

The two most common gas extraction techniques are heating in ultra-high vacuum using high-temperature vacuum ovens or lasers. Several laser extraction systems operating at 1064 (CW- and Q-switched modes), 533, 266, 193 nm, and vacuum furnaces with capacities ranging from 25 g to 10 mg were available for this work. However, we found that these options are not optimal for degassing sub-mg samples. Furnaces

typically have a high noble gas background, and laser extraction has poor temperature control, especially below ~800 °C.

Preparing mineral fractions from micro samples in an airless environment is not feasible. Therefore to separate gases released from various minerals, we employed step-wise gas extraction, taking advantage of the difference in thermal properties of the minerals involved. A miniaturized gas-extraction low-blank oven was built and calibrated up to 2000 °C for this work. This device was specifically developed to facilitate loading Ryugu samples without exposing them to the terrestrial atmosphere. An earlier version of this oven was used for analyses of noble gases from the 0.44 mg sample of IOM from the Paris meteorite.[25] The current version used in this work has an improved multilayer tantalum thermal shielding to homogenize temperature along the W-coil and all-metal sample loading device with custom made 6 mm thick sapphire viewport to observe manipulation of Pt-capsules containing micro-samples. This device was specifically developed to facilitate loading Ryugu samples without exposing them to the terrestrial atmosphere. The sample loading procedures along with sample weighting were performed in dry nitrogen, following the intricate protocol developed by Kyushu University (ref. 26 and 27).

Testing the experimental setup

To estimate the overall performance of our analytical setup, it would be reasonable to analyse noble gases extracted from a well-characterized, inter-laboratory standard that is homogeneous at sub-mg level. Unfortunately, except for Ar, no such standard exists to our knowledge. Instead, small calibrated shots of air are typically used as laboratory standards. However, a standard protocol has yet to be established for preparing, purifying, and admitting these air shots to the mass spectrometer. Pneumatically controlled valves commonly employed to "pipette" air standards into mass-spectrometers act too fast to completely avoid fractionation caused by molecular flow regime, with the extent of this fractionation depending on the internal volumes and conductance of a particular vacuum line.

Besides the extensive noble gas analyses of solid material returned from Ryugu,[26,27] JAXA collected the head gas accumulated in sample return capsules. Several well-equilibrated aliquots of this gas were prepared[28] and distributed among different laboratories, where they were independently analysed using different mass spectrometers and gas preparation techniques.[29] We will not discuss the results of these works here but rather consider the head gas sub-samples as a perfectly homogenized noble gas standard. Fig. 4 shows several noble gas isotopic ratios that include the least abundant isotopes. While the plotted ratios generally agree, 1σ error bars corresponding to ratios are different for the different experimental setups. Isotopic ratios obtained using Nier-type ion sources (Fig. 4a and d) are generally less precise compared to those from Baur sources (Fig. 4b and c).

Stability of the instruments with time

High ion transmission and the absence of a magnetic field in the ionisation region make sensitivity stable and less mass-dependent compared to the commercial mass-spectrometers equipped with the Nier-type ion source with an electron focusing magnet. The ring-shaped filament of the Baur ion source has a uniform temperature and provides nearly the same ionisation probability for each emitted electron. It is regulated by electron emission current, in contrast to electron trap current in the Nier-type source, which is typically a fraction of the emission current. This difference is likely the main reason for the long-time stability and reliability of the Baur source. The stability sensitivity and small and constant instrumental mass discrimination do not require frequent instrument calibration with air standards, saving time and reducing atmospheric memory. The ring filament operates at a relatively low temperature and lasts years, with little or no source retuning being needed after its replacement.

Our single collector instruments employ a stable, long-lasting Allen-type electron multiplier with Cu–BeO-dynodes. This alloy is known to provide a higher and more stable yield of secondary electrons than Al_2O_3, which is often preferred by electron multiplier manufacturers because of the concerns of beryllium toxicity.

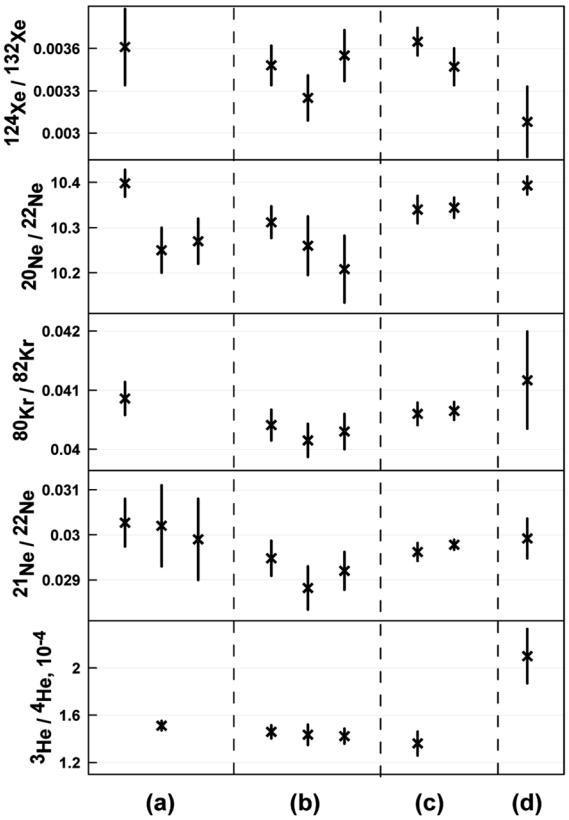

Fig. 4 Selected isotope ratios in the head gas from the Hayabusa2 sample return container, as measured by different laboratories employing different mass-spectrometry and noble gas extraction and purification techniques. Plotted data (from Table S1 in ESI,† ref. 29) were obtained using Nier-type ion source: at GRPG, Nancy (a); Kyushu Univ., Fukuoka (d) and Baur source: with reduced space charge effects at ETH, Zurich (b) and high transmission version at Washington Univ., St. Louis (c). Shown errors are 1σ.

Electronic units of our high ion transmission instruments are from reliable manufacturers: Spellman (Hauppauge, NY, USA), Stanford Research Systems (Sunnyvale, CA, USA), Bruker (Ettlingen, Germany), and Kepco Inc. (Flushing, NY, USA), with all of the units being controlled *via* GPIB using LabView (National Instrument, Austin, TX, USA) codes.

Results

Based on the on-hand comparison of several instruments and developmental work described above we have selected the best presently available for us technique for isotopic analyses of limited quantities of noble gases. It is the built in-house high sensitivity (5 mA $Torr^{-1}$ at 0.25 mA electron emission) 21 cm radius 90° magnetic sectors mass-spectrometer. This instrument is equipped with >90% ion transmission ion source without an e-focusing magnet and operates at the 3 kV acceleration voltage for Kr, Xe, and Ar and at 4 kV for light noble gases. This configuration results in low memory and long (>1 h. for Xe and Kr) useful ion-counting time (as Fig. 1 and 3 show). Instrumental mass discrimination is small (0.06%/u for Xe) and stable (*e.g.*, ref. 30). Sensitivity is stable, varies only few percent over a long time (see Fig. S2 in ESI†), and the instrument practically does not require retuning.

A miniature gas extraction low-blank oven was calibrated to ±15 °C. Chemically active gases were removed using a series of SEAS getters and freshly deposited Ti-films. A hot tungsten filament facilitated the cracking of complex hydrocarbons into fragments that more readily react with the getter material. Noble gases were separated cryogenically before the isotopic analyses into the fractions He + Ne, Ar, and Xe + Kr. Xe blank (1770 °C × 10 min) of ~3×10^{-15} cm^3 STP was determined by melting of Pt foil of the same weight as the Pt capsules containing actual samples.

We applied our developments for analyses of all noble gas isotopes from two Ryugu samples: A0105-04 (173 μg) and C0106-05 (82 μg), collected from the first and the second touchdown sites, respectively.[31] Ref. 26 and 32 report the preparation of the Ryugu samples and initial analyses. Gases were extracted in 7 temperature steps from C0106-05 and in 11 steps from A0105-04. Each extraction step lasted 10 minutes after the temperature reached the set point. Xe and Kr from A0105-04 suggest three major gas release peaks, while lower resolution step-heating of C0106-05 resolved only two peaks (Fig. 5).

Helium and neon

He ($m/z = 3$, 4) and Ne ($m/z = 20$, 21, 22) were not cryogenically separated from each other and analysed in one run along with peaks at $m/z = 2$, 18, 19, 40, 44 required for isobaric corrections that were applied individually within each mass scans. Blank corrections were applied using analyses of noble gases extracted from empty Pt-capsules identical to those containing actual samples. Isotopic compositions of He (Fig. 6) are consistent with pure and/or fractionated solar wind with possible minor contributions of He from phase Q at high temperatures. However, it is more likely that the apparent decrease in $^3He/^4He$ ratio with temperature results from a depth-dependent implantation effect, similar to the fractionation observed in Genesis solar wind collectors (Fig. 5a in ref. 15).

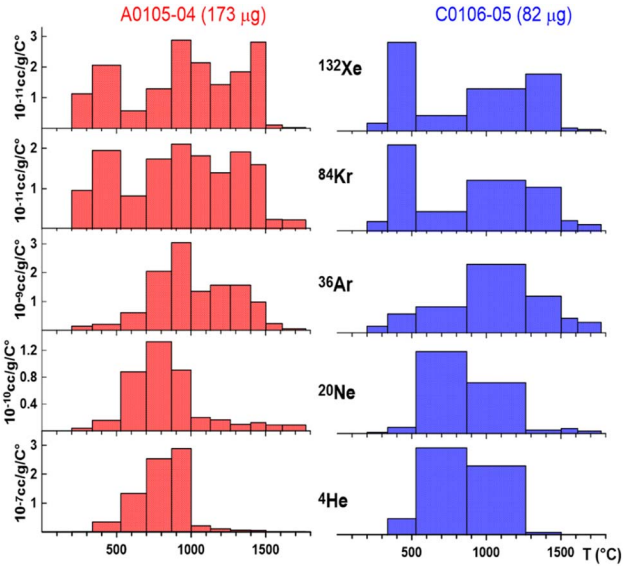

Fig. 5 Release profiles of the most abundant isotopes of noble gases released during step-wise heating from Ryugu samples collected from two different locations on the asteroid. Ordinates show temperature steps normalized to °C; therefore areas under the release curves accurately represent gas amounts.

Main Ne release occurs between 500 °C and 1260 °C. Neon released in this temperature interval is a mixture of solar wind, Q, and cosmogenic Ne, except for the 1260 °C extraction of the A0105-04 sample (Fig. 7).

Temperature fractions below ~900 °C are dominated by solar wind with a minor addition of cosmogenic Ne, which is somewhat smaller for C0106-05. Ne–Q dominates Ne at higher temperatures, with 1000–1300 °C being a typical destruction temperature of phase Q. At low and high temperatures, amounts of Ne released from both Ryugu samples only marginally exceed the blank level. The isotopic composition of

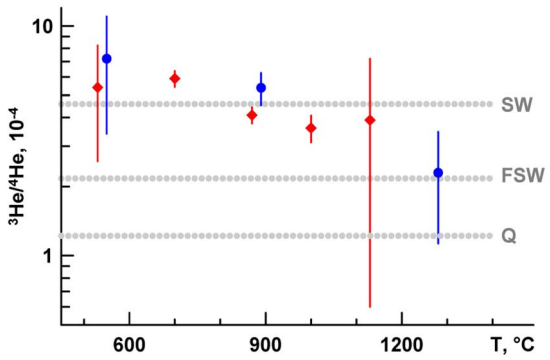

Fig. 6 Isotopic composition of helium released from Ryugu samples A0105-04 (red diamonds) and C0106-05 (blue circles). Dotted lines correspond to solar wind (SW), fractionated solar wind (FSW) and He associated with phase Q (P1).[16]

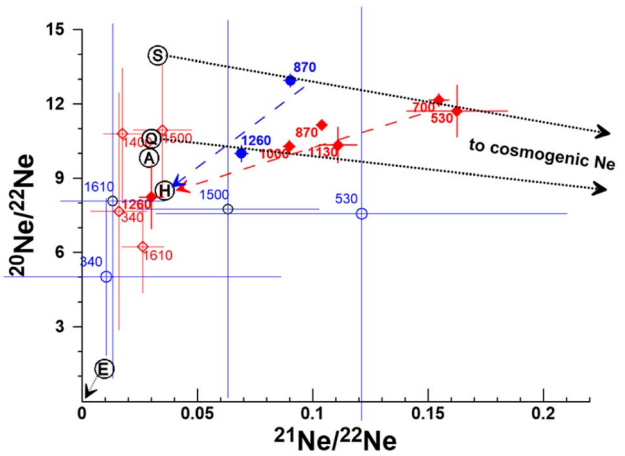

Fig. 7 Neon isotopes released from Ryugu samples A0105-04 (red diamonds) and C0106-05 (blue circles). Numbers indicate Ne extraction temperatures (in °C). Filled symbols and bold numbers correspond to the major gas release. Compositions of neon end-member components (S – Solar wind, Q – phase Q, A – atmospheric, H – neon-HL associated with meteoritic nanodiamonds, G – nearly pure ^{22}Ne produced in s-process and carried by SiC, and cosmogenic Ne) are from ref. 33–35. Dashed lines illustrate the trend of Ne isotopic composition during step-wise heating. As extraction temperature increases, Ne composition departs from the solar wind – cosmogenic mixing line towards Ne-HL. This trend is evident for A0105-04 (red) and suggestive for C0106-05 (blue). Errors are 1σ.

Ne in A0105-04 suggests the presence of Ne-HL, which is associated with meteoritic nanodiamonds. This component is not apparent in C0106-05, possibly due to the heterogeneous distribution of the Ne-HL component among ~100 μg grains. Neon released at 340 °C and 1610 °C from both samples tentatively show contribution from Ne–G associated with graphite and/or SiC; however, the large error bars (Fig. 7, further inflated after blank subtraction) prevent from this conclusion.

Argon

After He and Ne analyses, argon was further cryogenically separated from Kr and Xe and admitted to the mass spectrometer for analyses. In addition to Ar isotopes ($m/z = 36$, 38, 40), $m/z = 35$, 37 were also analyzed to correct for the ubiquitous $H^{35,37}Cl^+$. The interference corrections were applied for each of the twenty-five measurement cycles individually.

Argon is released from both Ryugu samples in one broad peak from ~400 °C to 1500 °C (Fig. 5). Within experimental uncertainties, $^{36}Ar/^{38}Ar$ ratios are uniform and close to solar wind Ar[35] at these temperatures, while outside this range, they are similar to Q and/or atmospheric values. There is neither indication of Ar-HL nor of cosmogenic argon. The latter is likely due to the low abundance of target elements in phase Q. If both Ryugu samples were similarly exposed to the solar wind, the A0105-04 apparently retains its signature better as suggested by temperature fractions below ~700 °C (Fig. 8).

Both samples contain highly variable amounts of ^{40}Ar. Well defined correlations of $^{38}Ar/^{40}Ar$ with $^{36}Ar/^{40}Ar$ yield the following values of $^{38}Ar/^{36}Ar$: 0.1833 ± 0.0054 (1σ) for C0106-05

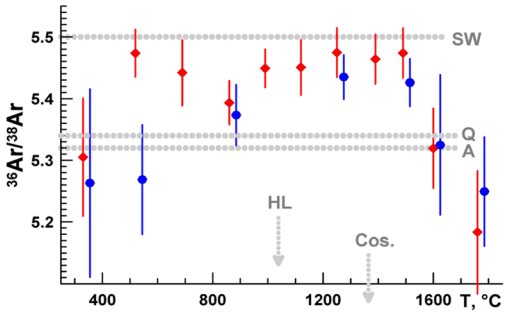

Fig. 8 Argon isotopes released from Ryugu samples A0105-04 (red diamonds) and C0106-05 (blue circles). End-member components (SW, A, Q, HL, and cosmogenic) are the same as in Fig. 7. Error bars are 1σ.

and 0.1840 ± 0.0009 (1σ) for A0105-04 (Fig. 9). The difference between these two values is statistically insignificant.

However, there is small but statistically significant difference in the y-intercepts of the fitting lines: (2.26 ± 0.84) × 10^{-5} for C0106-05 and (0.90 ± 0.55) × 10^{-5} for A0105-04. Both samples apparently have ^{38}Ar resolvable from zero at 1σ level, with C0106-05 having more cosmogenic ^{38}Ar contribution than A0105-04.

Krypton and xenon

It is difficult to estimate the contributions of solar and other Kr components, even for the most abundant isotopes, because of the relatively small isotopic differences in major Kr components. Krypton isotopic compositions that correspond to high-temperature fractions scatter within 1–2σ around atmospheric and Q values, while at temperatures below ~700 °C they are closer to the solar wind value (Fig. 10).

$^{86}Kr/^{84}Kr$ ratios in mid-temperature fractions (1000–1500 °C) are marginally elevated compared to Q-value, suggesting possible contributions from Kr-HL and/or Kr-G.

The three heaviest Xe isotopes ($m = 136$, 134, 132) are typically the most abundant and thus measured more precisely than other isotopes. However, the 3-isotope plot corresponding

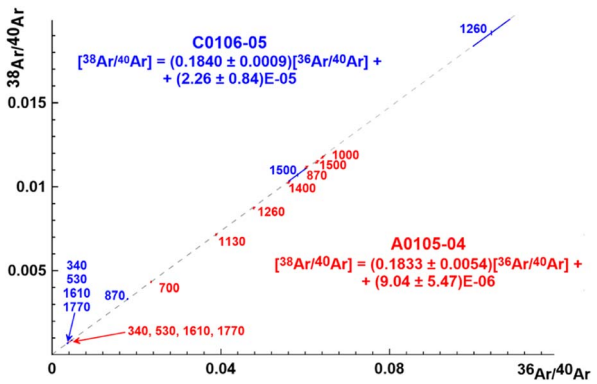

Fig. 9 Slopes of correlation lines between $^{38}Ar/^{40}Ar$ and $^{36}Ar/^{40}Ar$ suggests statistically insignificant difference in $^{38}Ar/^{36}Ar$ ratios in Ryugu samples A0105-04 and C0106-05.

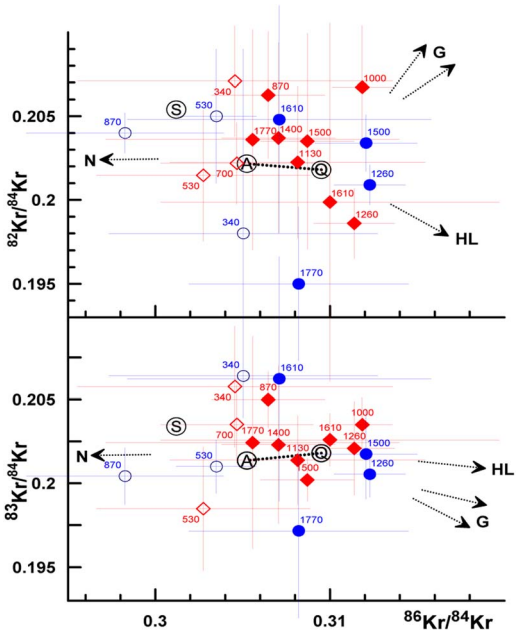

Fig. 10 Isotopic composition of Kr released from Ryugu samples A0105-04 (red diamonds) and C0106-05 (blue circles). Filled symbols correspond to temperature fractions above ~700 °C. End member components (S, A, Q, HL) are the same as in Fig. 7. Kr compositions of N and G (variable) carried by graphite or SiC are from ref. 33 and 34. Error bars are 1σ. Several points are slightly shifted (less that the symbol size) to improve clarity.

to these isotopes is probably the least diagnostic and is somewhat confusing (Fig. 11a). Generally all points representing our analyses scatter along the mixing line connecting atmospheric and Q values. Coincidently all other end members would shift experimental points along nearly the same line. Therefore, estimating relative contributions from potential Xe components based on this plot alone is nearly impossible. Three other more diagnostic Xe isotope plots are shown in Fig. 11b–d.

Total xenon extractions (*i.e.*, all temperature fractions combined) are plotted on the mixing line between atmospheric and Q (for clarity not depicted in Fig. 11). However, Xe extracted from 1260 °C to 1500 °C (typical range for Xe-HL) demonstrates small but statistically significant departures from Q-values (Fig. 11b and c). In contrast to lower temperature resolution laser gas extraction (ref. 22), the observed elevations in light isotopes ^{124}Xe, ^{126}Xe, ^{128}Xe, and possibly ^{129}Xe indicate the presence of Xe-HL – a presolar Xe component associated with nanodiamond in primitive meteorites. Neon released between 1130 °C and 1260 °C from sample A0105-04 also indicates the presence of an HL component; however, no Ne-HL is apparent in the C0106-05. This is likely due to the significantly lower temperature resolution of the C0106-05 gas extraction – the 1260 °C Ne extraction from this sample actually represents gas released from 870 °C to 1260 °C. All Xe plots combined reveal no evidences for Solar wind or Xe-G from SiC and graphite component.

Fig. 11d shows an excess of ^{129}Xe, evidently from the decay of primordial ^{129}I. Interestingly, this excess is observed from 870 °C to 1130 °C, in a narrower temperature range than for Xe-HL, reaching the maximum at 1000 °C extraction. This difference

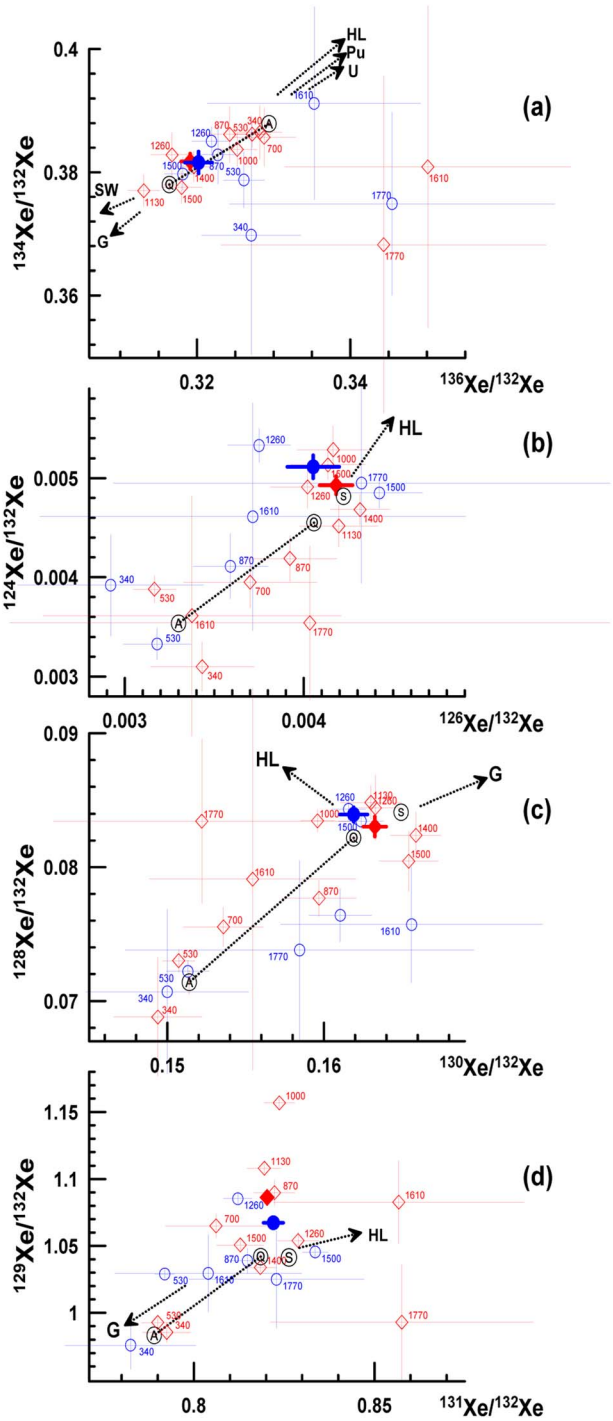

Fig. 11 Isotopic composition of Xe released from Ryugu samples A0105-04 (red diamonds) and C0106-05 (blue circles). Filled symbols correspond to Xe extracted from 1000 °C to 1500 °C for A0105-04 and from 1260 °C to 1500 °C for C0106-05. Fractions below 1000 °C tend to group close to the atmospheric value, while fractions above 1000 °C scatter around Q. End member components (SW, A, Q, HL, G) are the same as in the previous figures. Pu and U arrows show direction (from Q) to the corresponding fission compositions. Error bars are 1σ. Some points are shifted by the symbol size to improve clarity.

indicates that Xe-HL and iodine-derived Xe are carried by different mineral phases and step-wise gas extraction is capable of resolving them.

Discussion

Noble gases are retained in natural minerals surprisingly well and are released upon heating only when a host mineral is thermally destructed or goes through a major phase transition. Below ~900 °C, extraction of solar wind ions implanted in the outermost 1 μm grain layers typically occurs. The major noble gas component Q is released above ~1000 °C, and then, as temperature increases, HL (+P6) gases carried by the refractory carbon phase (nanodiamonds) appear. Radiogenic iodine-derived ^{129}Xe inherits its ^{129}I mother isotope site in the crystalline structure of the specific mineral and would be released in a temperature range characteristic of its host phase. Therefore, isotopic analyses of gases released during multistep heating can provide information about mineral phases that host released noble gas components.

The small mass of Ryugu material available for initial analyses limited the number of temperature steps. Recent studies of Ryugu noble gases[26,27] typically used 2–4 laser heating steps, which is not sufficient for satisfactory resolution of various noble gas components. We studied similarly sized samples, but our experimental setup allowed us to analyse all noble gas isotopes in 7 steps for the 82 μg sample (C0106-05) and 11 steps for the 173 μg sample (A0105-04) with the same or better precision. As evident from Fig. 1, seven heating steps were insufficient to resolve two the high-temperature Xe release peaks resolved in the 11-step gas extraction.

^{3}He/^{4}He ratios in both samples decrease with extraction temperature (Fig. 6), suggesting solar wind fractionation that increases with the implantation depth. Both samples have bulk ^{4}He/^{20}Ne ratios of 174 ± 5, lower than the solar wind value (~660) and closer to the Q value (~110). Therefore we cannot exclude a small contribution of He–Q.

Ne data (Fig. 7) exhibit an unmistakable low- and high-temperature component. The 530 °C and 700 °C extractions from A0105-04 are binary mixtures of solar wind and cosmogenic Ne. As the extraction temperature increases, the solar wind component is replaced by a mixture of Ne–Q (1000 °C) and cosmogenic Ne (1130 °C). The intermediate 870 °C extraction is a ternary mixture of solar wind, Q, and cosmogenic Ne components. The 1260 °C point suggests the presence of Ne-HL and indicates that the sample has already lost the solar wind and the cosmogenic Ne components. Two major Ne releases from sample C0106-05 demonstrate a similar trend; however, the 7-step extraction cannot resolve the presence of Ne-HL.

Argon likely has two major release peaks – below and above ~1000 °C (Fig. 5). From ~1000 °C to ~1500 °C the ^{36}Ar/^{38}Ar ratios in both samples are uniform and close to the solar wind value (Fig. 8). At the highest and the lowest temperatures, little Ar is released, and these ratios are consistent with both, Ar–Q and atmospheric values. The most noticeable variation in the ^{36}Ar/^{38}Ar ratios of the samples occurs during the gas release at low temperatures. In this temperature range C0106-05 has either more atmospheric Ar or more cosmogenic ^{38}Ar than A0105-04 or both. A good correlation between ^{36}Ar/^{40}Ar and ^{38}Ar/^{40}Ar (Fig. 9) suggests that ^{40}Ar is most likely from atmospheric contamination, not from the K-bearing minerals (^{40}Ar is negligible in the solar wind). There is no statistically significant difference between the correlation line slopes. However, a slight difference in the intercepts of the fitting lines with the ^{38}Ar/^{40}Ar axis supports a higher abundance of spallogenic ^{38}Ar in C0106-05. C0106-05 was collected during the second touchdown, about 20 m from the artificially created 1–2 m deep crater, and it was expected to contain some ejecta.[36] Since the production rate of ^{38}Ar increases with depth, a higher abundance of spallogenic ^{38}Ar in C0106-05 indicates that this sample represents a deeper layer of the asteroid.

Kr isotopic variations are relatively minor and typically less diagnostic for the presence of different noble gas components. Nevertheless, Kr isotopic compositions from low-temperature extractions tend to scatter around atmospheric values. At higher temperatures, they shift to Q-values with possible additions of Kr-HL and/or Kr-G (Fig. 10). This separation trend is more clearly observed in the Xe 3-isotope plots (Fig. 11).

Xe isotope plots are not equally informative. Although three heavy isotopes are typically measured with significantly better precision than the light ones, considering ^{134}Xe/^{132}Xe *vs.* ^{136}Xe/^{132}Xe (Fig. 11a) alone can be misleading since nearly all Xe components lie along the same mixing line between Q and atmospheric values. Light, least abundant, isotopes are measured with significantly lower precision. Nevertheless, the ^{124}Xe/^{132}Xe *vs.* ^{126}Xe/^{132}Xe experimental points represent a high-temperature release peak that indicates enrichment in ^{124}Xe and ^{126}Xe. This result is consistent with Xe-HL, the only known Xe component that can produce the observed shift from Xe–Q (Fig. 11b). The small excess of ^{128}Xe, also a characteristic feature of Xe-HL, is apparent in ^{128}Xe/^{132}Xe *vs.* ^{130}Xe/^{132}Xe (Fig. 11c). Although Xe-G is also enriched in ^{128}Xe, this excess is unlikely due to the presence of presolar SiC or graphite since they are less abundant then nanodiamonds, the carrier of Xe-HL. Considering all the noble gas isotopes together, our data confirm the presence of the HL component in both samples analysed in this work, hence, resolving the doubts about its presence in Ryugu samples.[27]

Xe plot involving odd isotopes (Fig. 11d) shows clear excess of ^{129}Xe, the decay product of extinct ^{129}I (15.6 Myr), with ^{129}Xe being released in a more narrow temperature range than Xe–Q, suggesting different host minerals for these two components. A close relationship between Ryugu and CI chondrites was previously suggested based on the nitrogen and noble gases data.[27] Interestingly, the release of radiogenic iodine-derived ^{129*}Xe in magnetite separated from CI carbonaceous chondrite Orgueil is characterized by two major peaks;[37] the low temperature one in a 900–1050 °C range, similar to what is observed here for the Ryugu samples. The presence of magnetite is a marker of aqueous activity. Based on the ^{53}Mn–^{53}Cr systematics of Ryugu carbonates, the fluid–rock interaction occurred within approximately the first 2–5 million years of solar system history.[38,39] Since magnetite is one of the first minerals to form during aqueous alteration, studding Xe isotopic systematics in magnetite separated from Ryugu could further refine the alteration timeline.

Conclusions

Superior ion utilization in Baur ion source, relatively low mass-spectrometer volume, very small, stable instrumental mass-discrimination, low memory and background achieved in our experimental setup allow retrieving more information from the sub-mg amounts of extraterrestrial material and separation of noble gas components by applying multi-step gas extraction techniques. Particularly, some doubts about the presence of apparently presolar xenon-HL have been resolved. Presence of radiogenic iodine-derived ^{129*}Xe in the Ryugu samples in a temperature range observed for the CI chondrite Orgueil, further support the relationship between Ryugu in CI chondrites.

Author contributions

Al. M. and O. P. made analytical developments, performed analyses of asteroid samples delivered by the Hayabusa2 mission and prepared first version of the manuscript. R. O., K. S. and Sh. T. developed novel techniques to collect samples from the asteroid surface, to protect them from atmospheric contamination (for the first time since the beginning of sample return era). R. O., F. K. and T. Y. prepared the samples for the noble gas analysis. H. Y., To. N, Ta. N., R. O., H. Y., H. N., K. S. and S. T. coordinated the Ryugu sample initial analysis campaign. K. Y., T. Y., M. N., A. N., Ak. M., M. A., T. O. and T. U. contributed the Ryugu sample curation at JAXA. M. Y., T. S., Sa. T., F. T., S. N., S. W. and Y. T. oversaw the entire operation phase of the spacecraft including two sampling operations.

Conflicts of interest

There are no conflicts to declare.

Acknowledgements

We are grateful to Dr Charles Hohenberg, the founder of noble gas facility at Physics Department of Washington University, who recognised early on the analytical potential of the Baur ion source and built the first mass-spectrometer equipped with this source. John Stehman helped to write a LabView code to control the mass spectrometer used in this study. Hayabusa2 YAXA mission provided unique samples and developed intricate technique to avoid atmospheric contamination after landing. We thank Jeffrey Gillis-Davis for his help with revising the manuscript and the anonymous reviewers for their valuable comments and suggestions. This work is supported by NASA grants 80NSSC22K0590, 80NSSC17K0018 and JAXA Hayabusa2 mission.

References

1 M. Ozima and F. A. Podosek, *Noble Gas Geochemistry*, Cambridge University Press, Cambridge, 2nd edn, 2002.
2 R. S. Lewis, B. Srinivasan and E. Anders, Host Phase of a Strange Xenon Component in Allende, *Science*, 1975, **190**, 1251–1262.
3 U. Ott, Planetary and pre-solar noble gases in meteorites, *Chem. Erde*, 2014, **74**(4), 519–544.
4 H. Y. McSween Jr. and G. R. Huss, *Cosmochemistry*, Cambridge University Press, 2010, p. 568, ISBN 978-0-521-87862-3.
5 R. S. Lewis, S. Amari and E. Anders, Interstellar grains in meteorites: II. SiC and its noble gases, *Geochim. Cosmochim. Acta*, 1994, **58**, 471–494.
6 R. Wieler, Noble Gas Mass Spectrometry, in, *Treatise on Geochemistry*, Elsevier, Oxford, 2nd edn, 2014, vol. 15, pp. 355–373. DOI: 10.1016/B978-0-08-095975-7.01428-5.
7 A. Meshik and O. Pravdivtseva, Noble gas laboratory at Washington University: history and analytical capabilities, *47th Lunar and Planetary Science Conference*, 2016, p. 1681, https://www.hou.usra.edu/meetings/lpsc2016/pdf/1681.pdf.
8 C. M. Hohenberg, *Rev. Sci. Instrum.*, 1980, **51**(8), 1075–1082.
9 S. A. Crowther and J. D. Gilmour, *J. Anal. At. Spectrom.*, 2012, **27**, 256–269.
10 I. Strashnov, D. J. Blagburn and J. D. Gilmour, A resonance ionization time of flight mass spectrometer with a cryogenic sample concentrator for isotopic analysis of krypton from extraterrestrial samples, *J. Anal. At. Spectrom.*, 2011, **26**, 1763–1772.
11 G. Avice, A. Belousov, K. A. Farle, S. M. Madzunkov, J. Simcic, D. Nikolic, M. R. Darrach and C. Sotin, High-precision measurements of krypton and xenon isotopes with a new static-mode Quadrupole Ion Trap Mass Spectrometer, *J. Anal. At. Spectrom.*, 2019, **34**, 104.
12 H. Baur, Numerische Simulation und Praktische Erprobung einer Rotation-Symmetrischen Ionenquelle für Gasmassenspektrometer, *PhD thesis*, ETH Zürich, 1980, p. 94, Nr. 6596.
13 F. Albarède, E. Albalat and P. Télouk, Instrumental Isotope Fractionation in Multiple-Collector ICP-MS, *J. Anal. At. Spectrom.*, 2015, **30**, 1736–1742.
14 N. Vogel, V. S. Heber, H. Baur, D. S. Burnett and R. Wieler, Argon, krypton, and xenon in the bulk solar wind as collected by the Genesis mission, *Geochim. Cosmochim. Acta*, 2011, **75**, 3057–3071.
15 A. Meshik, C. Hohenberg, O. Pravdivtseva and D. Burnett, Measuring the isotopic composition of solar wind noble gases, in *Exploring the Solar Wind*, ed. M. Lasar, InTech, 2012, pp. 93–121, ISBN 978-953-51-0339-4, https://www.intechopen.com/chapters/32533.
16 U. Ott, B. Baecker and M. Trieloff, Multiple ion counting in noble gas mass spectrometry, *Workshop on the Modern Analytical Methods Applied to Earth and Planetary Sciences*, Sopron, Hungary, 2014, LPI Contribution No. 1821, id.4001.
17 S. E. Cox, S. R. Hemming and D. Tootell, The Isotopx NGX and ATONA Faraday amplifiers, *Geochronology*, 2020, **2**, 231–243, DOI: 10.5194/gchron-2-231-2020.
18 Z. A. Palacz, *High Precision Calcium Isotope Ratio Measurements Using Faraday Collectors with ATONA Amplifiers*, American Geophysical Union, Fall Meeting, 2018, abstract #V43A-01, Bibcode: 2018AGUFM.V43A.01P.
19 R. Moshammer and R. Matthäus, Secondary electron emission by low energy ion impact, *J. Phys., Colloq.*, 1989, **50**(C2), 111–120, DOI: 10.1051/jphyscol:1989220.

20 C. M. Hohenberg, N. Thonnard and A. Meshik, *Meteorit. Planet. Sci.*, 2002, **37**, 257–267, DOI: **10.1111/j.1945-5100.2002.tb01108.x**.

21 R. Okazaki, H. Sawada, S. Yamanouchi, Sh. Tachibana, Y. N. Miura, K. Sakamoto, Y. Takano, M. Abe, S. Itoh, K. Yamada, H. Yabuta, C. Okamoto, H. Yano, T. Noguchi, T. Nakamura, K. Nagao and The Hayabusa2 SMP Team, Hayabusa2 Sample Catcher and Container: Metal-Seal System for Vacuum Encapsulation of Returned Samples with Volatiles and Organic Compounds Recovered from C-Type Asteroid Ryugu, *Space Sci. Rev.*, 2017, **208**, 107–124, DOI: **10.1007/s11214-016-0289-5**.

22 H. Sawada, R. Okazaki, S. Tachibana, K. Sakamoto, Y. Takano, C. Okamoto, H. Yano, Y. Miura, M. Abe, S. Hasegawa, T. Noguchi and Hayabusa2 SMP Team, Hayabusa2 Sampler: Collection of Asteroidal Surface Material, *Sci. Rev.*, 2017, **208**, 81–106, DOI: **10.1007/s11214-017-0338-8**.

23 K. Sakamoto, Y. Takano, H. Sawada, R. Okazaki, T. Noguchi, M. Uesugi, H. Yano, T. Yada, M. Abe, S. Tachibana and The Hayabusa2 Project Team, Environmental assessment in the prelaunch phase of Hayabusa2 for safety declaration of returned samples from the asteroid (162173) Ryugu: background monitoring and risk management during development of the sampler system, *Earth, Planets Space*, 2022, **74**, 90, DOI: **10.1186/s40623-022-01628-z**.

24 A. Meshik, C. M. Hohenberg, O. Pravdivtseva and D. S. Burnett, *Geochim. Cosmochim. Acta*, 2014, **127**, 326–347.

25 D. V. Bekaert, Y. Marrocchi, A. Meshik, L. Remusat and B. Marty, *Meteorit. Planet. Sci.*, 2019, **54**, 395–414, DOI: **10.1111/maps.13213**.

26 R. Okazaki, B. Marty, H. Busemann, K. Hashizume, J. D. Gilmour, A. Meshik, T. Yada, F. Kitajima, M. W. Broadle, D. Byrne, E. Füri, M. E. I. Riebe, D. Krietsch, C. Maden, A. Ishida, P. Clay, S. A. Crowther, L. Fawcett, T. Lawton, O. Pravdivtseva, Y. N. Miura, J. Park, K. Bajo, Y. Takano, K. Yamada, S. Kawagucci, Y. Matsui, M. Yamamoto, K. Righter, S. Sakai, N. Iwata, N. Shirai, S. Sekimoto, M. Inagaki, M. Ebihara, R. Yokochi, K. Nishiizumi, K. Nagao, J. Lee, A. Kano, M. W. Caffee, R. Uemura, T. Nakamura, H. Naraoka, T. Noguchi, H. Yabuta, H. Yurimoto, S. Tachibana, H. Sawada, K. Sakamoto, M. Abe, M. Arakawa, A. Fujii, M. Hayakawa, N. Hirata, N. Hirata, R. Honda, Ch. Honda, S. Hosoda, Y. Iijima, H. Ikeda, M. Ishiguro, Y. Ishihara, T. Iwata, K. Kawahara, S. Kikuchi, K. Kitazato, K. Matsumoto, M. Matsuoka, T. Michikami, Y. Mimasu, A. Miura, T. Morota, S. Nakazawa, N. Namiki, H. Noda, R. Noguchi, N. Ogawa, K. Ogawa, T. Okada, C. Okamoto, G. Ono, M. Ozaki, T. Saiki, N. Sakatani, H. Senshu, Y. Shimaki, K. Shirai, S. Sugita, Yu. Takei, H. Takeuchi, S. Tanaka, E. Tatsumi, F. Terui, R. Tsukizaki, K. Wada, M. Yamada, T. Yamada, Y. Yamamoto, H. Yano, Y. Yokota, K. Yoshihara, M. Yoshikawa, K. Yoshikawa, S. Furuya, K. Hatakeda, T. Hayashi, Y. Hitomi, K. Kumagai, A. Miyazaki, A. Nakato, M. Nishimura, H. Soejima, A. Iwamae, D. Yamamoto, K. Yogata, M. Yoshitake, R. Fukai, T. Usui, H. C. Connolly Jr, D. Lauretta, S. Watanabe and Y. Tsuda, Noble gases and nitrogen in samples of asteroid Ryugu record its volatile sources and recent surface evolution, *Science*, 2022, **379**(6634), eabo0431, DOI: **10.1126/science.abo0431**.

27 M. W. Broadley, D. J. Byrne, E. Füri, L. Zimmermann, B. Marty, R. Okazaki, T. Yada, F. Kitajima, S. Tachibana, K. Yogata, K. Sakamoto, H. Yurimoto, T. Nakamura, T. Noguchi, H. Naraoka, H. Yabuta, S. Watanabe, Y. Tsuda, M. Nishimura, A. Nakato, A. Miyazaki, M. Abe, T. Okada, T. Usui, M. Yoshikawa, T. Saiki, S. Tanaka, F. Terui, S. Nakazawa, H. Busemann, K. Hashizume, J. D. Gilmour, A. Meshik, M. E. I. Riebe, D. Krietsch, C. Maden, A. Ishida, P. Clay, S. A. Crowther, L. Fawcett, T. Lawton, O. Pravdivtseva, Y. N. Miura, J. Park, K. Bajo, Y. Takano, K. Yamada, S. Kawagucci, Y. Matsui, M. Yamamoto, K. Righter, S. Sakai, N. Iwata, N. Shirai, S. Sekimoto, M. Inagaki, M. Ebihara, R. Yokochi, K. Nishiizumi, K. Nagao, J. I. Lee, A. Kano, M. W. Caffee and R. Uemura, The noble gas and nitrogen relationship between Ryugu and carbonaceous chondrites, *Geochim. Cosmochim. Acta*, 2023, **345**, 62–73, DOI: **10.1016/j.gca.2023.01.020**.

28 Y. N. Miura, R. Okazaki, Y. Takano, K. Sakamoto, Sh. Tachibana, K. Yamada, S. Sakai and H. Sawada, The GAs Extraction and Analyses system (GAEA) for immediate extraction and measurements of volatiles in the Hayabusa2 sample container, *Earth, Planets Space*, 2022, **74**, 76, DOI: **10.1186/s40623-022-01638-x**.

29 R. Okazaki, Y. N. Miura, Y. Takano, H. Sawada, K. Sakamoto, T. Yada, K. Yamada, S. Kawagucci, Y. Matsui, K. Hashizume, A. Ishida, M. W. Broadley, B. Marty, D. Byrne, E. Füri, A. Meshik, O. Pravdivtseva, H. Busemann, M. E. I. Riebe, J. Gilmour, J. Park, K. Bajo, K. Righter, S. Sakai, S. Sekimoto, F. Kitajima, S. A. Crowther, N. Iwata, N. Shirai, M. Ebihara, R. Yokochi, K. Nishiizumi, K. Nagao, J. Ik Lee, P. Clay, A. Kano, M. W. Caffee, R. Uemura, M. Inagaki, D. Krietsch, C. Maden, M. Yamamoto, L. Fawcett, T. Lawton, T. Nakamura, H. Naraoka, T. Noguchi, H. Yabuta, H. Yurimoto, Y. Tsuda, S. Watanabe, M. Abe, M. Arakawa, A. Fujii, M. Hayakawa, N. Hirata, N. Hirata, R. Honda, C. Honda, S. Hosoda, Y. Iijima, H. Ikeda, M. Ishiguro, Y. Ishihara, T. Iwata, K. Kawahara, S. Kikuchi, K. Kitazato, K. Matsumoto, M. Matsuoka, T. Michikami, Y. Mimasu, A. Miura, T. Morota, S. Nakazawa, N. Namiki, H. Noda, R. Noguchi, N. Ogawa, K. Ogawa, T. Okada, C. Okamoto, G. Ono, M. Ozaki, T. Saiki, N. Sakatani, H. Senshu, Y. Shimaki, K. Shirai, S. Sugita, Y. Takei, H. Takeuchi, S. Tanaka, E. Tatsumi, F. Terui, R. Tsukizaki, K. Wada, M. Yamada, T. Yamada, Y. Yamamoto, H. Yano, Y. Yokota, K. Yoshihara, M. Yoshikawa, S. Furuya, K. Hatakeda, T. Hayashi, Y. Hitomi, K. Kumagai, A. Miyazaki, A. Nakato, M. Nishimura, H. Soejima, A. Iwamae, D. Yamamoto, K. Yogata, M. Yoshitake, R. Fukai, T. Usui, T. Ireland, H. C. Connolly Jr, D. S. Lauretta and S. Tachibana, First asteroid gas sample delivered by the Hayabusa2 mission: A

treasure box from Ryugu, *Sci. Adv.*, 2022, **8**, eabo7239, DOI: 10.1126/sciadv.abo7239.

30 O. Pravdivtseva, F. L. H. Tissot, N. Dauphas and S. Amari, Evidence of presolar SiC in the Allende Curious Marie calcium–aluminium-rich inclusion, *Nat. Astron.*, 2020, **4**, 617–624.

31 T. Morota, S. Sugita, Y. Cho, M. Kanamaru, E. Tatsumi, N. Sakatani, R. Honda, N. Hirata, H. Kikuchi, M. Yamada, Y. Yokota, S. Kameda, M. Matsuoka, H. Sawada, C. Honda, T. Kouyama, K. Ogawa, H. Suzuki, K. Yoshioka, M. Hayakawa, N. Hirata, M. Hirabayashi, H. Miyamoto, T. Michikami, T. Hiroi, R. Hemmi, O. S. Barnouin, C. M. Ernst, K. Kitazato, T. Nakamura, L. Riu, H. Senshu, H. Kobayashi, S. Sasaki, G. Komatsu, N. Tanabe, Y. Fujii, T. Irie, M. Suemitsu, N. Takaki, C. Sugimoto, K. Yumoto, M. Ishida, H. Kato, K. Moroi, D. Domingue, P. Michel, C. Pilorget, T. Iwata, M. Abe, M. Ohtake, Y. Nakauchi, K. Tsumura, H. Yabuta, Y. Ishihara, R. Noguchi, K. Matsumoto, A. Miura, N. Namiki, S. Tachibana, M. Arakawa, H. Ikeda, K. Wada, T. Mizuno, C. Hirose, S. Hosoda, O. Mori, T. Shimada, S. Soldini, R. Tsukizaki, H. Yano, M. Ozaki, H. Takeuchi, Y. Yamamoto, T. Okada, Y. Shimaki, K. Shirai, Y. Iijima, H. Noda, S. Kikuchi, T. Yamaguchi, N. Ogawa, G. Ono, Y. Mimasu, K. Yoshikawa, T. Takahashi, Y. Takei, A. Fujii, S. Nakazawa, F. Terui, S. Tanaka, M. Yoshikawa, T. Saiki, S. Watanabe and Y. Tsuda, Sample collection from asteroid (162173) Ryugu by Hayabusa2: Implications for surface evolution, *Science*, 2020, **368**(6491), 654–659, DOI: 10.1126/science.aaz6306.

32 R. Okazaki, S. Yamanouchi, K. Shimada, A. Baba, F. Kitajima and T. Yada, Methods and tools for handling, transportation, weighing, and pelletization applied to the initial analysis of volatile components in the Hayabusa2 samples, *Earth, Planets Space*, 2022, **74**, 190, DOI: 10.1186/s40623-022-01747-7.

33 G. R. Huss, A. P. Meshik, J. B. Smith and C. M. Hohenberg, Presolar diamond, silicon carbide, and graphite in carbonaceous chondrites: implications for thermal processing in the solar nebula, *Geochim. Cosmochim. Acta*, 2003, **67**(24), 4823–4848, DOI: 10.1016/j.gca.2003.07.019.

34 R. S. Lewis, B. Srinivasan and E. Anders, Host phase of a strange xenon component in Allende, *Science*, 1975, **190**, 1251–1262.

35 A. Meshik, J. Mabry, C. Hohenberg, Y. Marrocchi, O. Pravdivtseva, D. Burnett, C. Olinger, D. Reisenfeld and A. J. G. Jurewicz, Constraints on neon and argon isotopic fractionation in solar wind, *Science*, 2007, **318**, 433–435, DOI: 10.1126/science.1145528.

36 S. Tachibana, H. Sawada, R. Okazaki, Y. Takano, K. Sakamoto, Y. N. Miura, C. Okamoto, H. Yano, S. Yamanouchi, P. Michel, Y. Zhang, S. Schwartz, F. Thuillet, H. Yurimoto, T. Nakamura, T. Noguchi, H. Yabuta, H. Naraoka, A. Tsuchiyama, N. Imae, K. Kurosawa, A. M. Nakamura, K. Ogawa, S. Sugita, T. Morota, R. Honda, S. Kameda, E. Tatsumi, Y. Cho, K. Yoshioka, Y. Yokota, M. Hayakawa, M. Matsuoka, N. Sakatani, M. Yamada, T. Kouyama, H. Suzuki, C. Honda, T. Yoshimitsu, T. Kubota, H. Demura, T. Yada, M. Nishimura, K. Yogata, A. Nakato, M. Yoshitake, A. I. Suzuki, S. Furuya, K. Hatakeda, A. Miyazaki, K. Kumagai, T. Okada, M. Abe, T. Usui, T. R. Ireland, M. Fujimoto, T. Yamada, M. Arakawa, H. C. Connolly Jr, A. Fujii, S. Hasegawa, N. Hirata, N. Hirata, C. Hirose, S. Hosoda, Y. Iijima, H. Ikeda, M. Ishiguro, Y. Ishihara, T. Iwata, S. Kikuchi, K. Kitazato, D. S. Lauretta, G. Libourel, B. Marty, K. Matsumoto, T. Michikami, Y. Mimasu, A. Miura, O. Mori, K. Nakamura-Messenger, N. Namiki, A. N. Nguyen, L. R. Nittler, H. Noda, R. Noguchi, N. Ogawa, G. Ono, M. Ozaki, H. Senshu, T. Shimada, Y. Shimaki, K. Shirai, S. Soldini, T. Takahashi, Y. Takei, H. Takeuchi, R. Tsukizaki, K. Wada, Y. Yamamoto, K. Yoshikawa, K. Yumoto, M. E. Zolensky, S. Nakazawa, F. Terui, S. Tanaka, T. Saiki, M. Yoshikawa, S. Watanabe and Y. Tsuda, Pebbles and sand on asteroid (162173) Ryugu: In situ observation and particles returned to Earth, *Science*, 2022, **375**, 1011–1016, DOI: 10.1126/science.abj8624.

37 O. Pravdivtseva, A. N. Krot and C. M. Hohenberg, I-Xe dating of aqueous alteration in the CI chondrite Orgueil: I. Magnetite and ferromagnetic separates, *Geochim. Cosmochim. Acta*, 2018, **227**, 38–47, DOI: 10.1016/j.gca.2018.02.004.

38 K. A. McCain, N. Matsuda, M.-C. Liu, K. D. McKeegan, A. Yamaguchi, M. Kimura, N. Tomioka, M. Ito, N. Imae, M. Uesugi, N. Shirai, T. Ohigashi, R. C. Greenwood, K. Uesugi, A. Nakato, K. Yogata, H. Yuzawa, Y. Kodama, K. Hirahara, I. Sakurai, I. Okada, Y. Karouji, S. Nakazawa, T. Okada, T. Saiki, S. Tanaka, F. Terui, M. Yoshikawa, A. Miyazaki, M. Nishimura, T. Yada, M. Abe, T. Usui, S. Watanabe and Y. Tsuda, Early fluid activity on Ryugu inferred by isotopic analyses of carbonates and magnetite, *Nat. Astron.*, 2023, **7**, 309–317. https://www.nature.com/articles/s41550-022-01863-0.

39 T. Yokoyama, K. Nagashima, I. Nakai, E. D. Young, Y. Abe, J. Aléon, C. M. O. 'D. Alexander, S. Amari, Y. Amelin, K. Bajo, M. Bizzarro, A. Bouvier, R. W. Carlson, M. Chaussidon, B.-G. Choi, N. Dauphas, A. M. Davis, T. Di Rocco, W. Fujiya, R. Fukai, I. Gautam, M. K. Haba, Y. Hibiya, H. Hidaka, H. Homma, P. Hoppe, G. R. Huss, K. Ichida, T. Iizuka, T. R. Ireland, A. Ishikawa, M. Ito, S. Itoh, N. Kawasaki, N. T. Kita, K. Kitajima, T. Kleine, S. Komatani, A. N. Krot, M.-C. Liu, Y. Masuda, K. D. McKeegan, M. Morita, K. Motomura, F. Moynier, A. Nguyen, L. Nittler, M. Onose, A. Pack, C. Park, L. Piani, L. Qin, S. S. Russell, N. Sakamoto, M. Schönbächler, L. Tafla, H. Tang, K. Terada, Y. Terada, T. Usui, S. Wada, M. Wadhwa, R. J. Walker, K. Yamashita, Q.-Z. Yin, S. Yoneda, H. Yui, A.-C. Zhang, H. C. Connolly Jr, D. S. Lauretta, T. Nakamura, H. Naraoka, T. Noguchi, R. Okazaki, K. Sakamoto, H. Yabuta, M. Abe, M. Arakawa, A. Fujii, M. Hayakawa, N. Hirata, Na. Hirata, R. Honda, Ch. Honda, S. Hosoda, Y. Iijima, H. Ikeda, M. Ishiguro, Y. Ishihara, T. Iwata, K. Kawahara, S. Kikuchi, K. Kitazato,

K. Matsumoto, M. Matsuoka, T. Michikami, Y. Mimasu, A. Miura, T. Morota, S. Nakazawa, N. Namiki, H. Noda, R. Noguchi, N. Ogawa, K. Ogawa, T. Okada, Ch. Okamoto, G. Ono, M. Ozaki, T. Saiki, N. Sakatani, H. Sawada, H. Senshu, Y. Shimaki, K. Shirai, S. Sugita, Y. Takei, H. Takeuchi, S. Tanaka, E. Tatsumi, F. Terui, Y. Tsuda, R. Tsukizaki, K. Wada, S. ichiro Watanabe, M. Yamada, T. Yamada, Y. Yamamoto, H. Yano, Y. Yokota, K. Yoshihara, M. Yoshikawa, K. Yoshikawa, S. Furuya, K. Hatakeda, T. Hayashi, Y. Hitomi, K. Kumagai, A. Miyazaki, A. Nakato, M. Nishimura, H. Soejima, A. Suzuki, T. Yada, D. Yamamoto, K. Yogata, M. Yoshitake, S. Tachibana and H. Yurimoto, Samples returned from the asteroid Ryugu are similar to Ivuna-type carbonaceous meteorites, *Science*, 2022, **379**, 6634, DOI: **10.1126/science.abn7850**.